

## Tuning the focus of a plasmonic lens by the incident angle

Zhaowei Liu, Jennifer M. Steele,<sup>a)</sup> Hyesog Lee, and Xiang Zhang<sup>b)</sup>  
*National Science Foundation, Nano-scale Science and Engineering Center (NSEC),  
 5130 Etcheverry Hall, University of California, Berkeley, California 94720-1740*

(Received 1 November 2005; accepted 22 February 2006; published online 27 April 2006)

We report the experimental realization of tuning the focus position of a plasmonic lens by adjusting the angle of the incident light similar to conventional lenses. A circular slit in silver film acts as both a surface plasmon polariton coupler and a plasmonic focusing lens. At small incident angles, the plasmonic lens has a very good focus with the position depending only on the angle of the incident beam. Numerical simulations of the focusing properties, including polarization dependence, agree well with experimental observations. This tunable plasmonic lens can be used in nanoscale photonics, biological sensing, and manipulation. © 2006 American Institute of Physics.  
 [DOI: 10.1063/1.2188378]

Surface plasmon polaritons (SPPs) have been of interest to various fields for many decades. Recent advances have allowed metallic structures to be used as subwavelength optical devices essential for downsizing future integrated optical circuits.<sup>1</sup> Various plasmonic elements are needed in this area to achieve SPP conversion from free-space photons as well as comprehensive controls of SPPs at subwavelength scale. Many elements, such as mirrors, lenses, waveguides, beam splitters, beam profilers, and interferometers have already been demonstrated.<sup>2–12</sup> In this letter, we present a method to tune the focal position of a plasmonic lens and experimentally investigate the tunability and focusing properties. A narrow slit in a metallic film can be used to couple free-space light into SPPs.<sup>11</sup> The diffracted light from the slit gains additional wave vector ( $\Delta k$ ) along the film surface, allowing a portion of the incident light to excite SPPs. Even though the coupling efficiency of a slit is lower than that of a grating, the slit has its own advantage in that it can couple light of different frequencies. The slit can be modeled as a collection of SPP point sources of which the wave vectors at the metal/dielectric interface are selected according to its dispersion curve.<sup>13</sup>

If normally incident free-space light is used for excitation [Fig. 1(a)], the in-plane wave vector will come entirely from the diffraction of light resulting from the slit. The direction of the generated SPP wave vector, which determines the energy propagation direction, will be perpendicular to the slit. Consequently, in the case of a circular slit, or plasmonic lens, the energy will be guided toward the center of the circle [Fig. 1(c)]. The focus of intensity dependence on the diameter of the plasmonic lens was studied in our previous paper.<sup>11</sup>

If the incident excitation light is inclined at an angle  $\theta$  [Fig. 1(b)], it carries the in-plane wave vector component of  $k_{in} = k_0 \sin(\theta)$ , where  $k_0$  is the free-space wave vector. Because of in-plane momentum conservation, this extra component will influence the excited SPP wave vector ( $k_{sp}$ ) direction,<sup>14</sup> but not the wave vector magnitude, which is determined only by the dispersion curve. The new  $k_{sp}$  will not

point to the center of the circle, but will shift by the direction of  $k_{in}$ . As the vector notation indicates in Fig. 1(d), from an arbitrary point A on the circumference of the slit, the SPP is guided to point B as opposed to the circle center. With the fixed magnitude of  $k_{sp}$ , the fixed direction and magnitude of  $k_{in}$  with given illumination configuration, and the fixed direction of the  $k$  vector provided by the slit (always pointing to the circle center), the displacement  $x$  defined as the distance from the circle center to point B in Fig. 1(d) is determined by the following relation:

$$x^2 \left( \frac{k_{sp}^2}{k_{in}^2} - 1 \right) = R^2 - 2Rx \cos \alpha, \quad (1)$$

where  $R$  is the radius of the lens and  $\alpha$  is an arbitrary angle that depends on the position of point A. If  $x$  is much smaller than  $R$ , the term  $-2Rx \cos \alpha$  is negligible, so Eq. (1) can be rewritten as

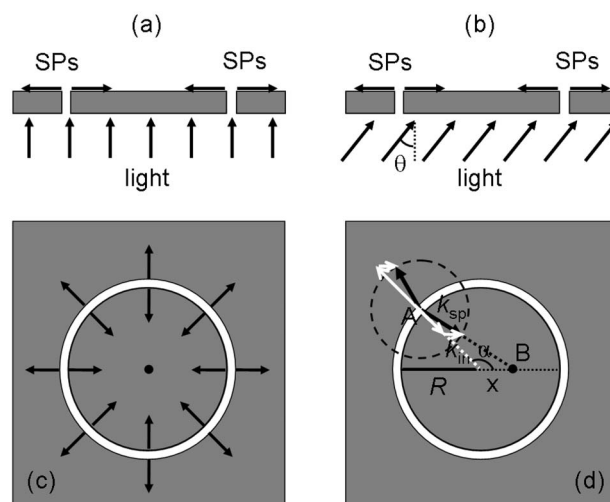


FIG. 1. Sketch of a plasmonic lens under (a) normal and (b) inclined illumination. (c),(d) top view of (a) and (b), respectively. (c) The focus (black dot) of the plasmonic lens is the center of the circle under normal illumination. (d) The focus (point B) of the plasmonic lens shifts away from the center under inclined illumination. The amount of shifted distance depends on the size of the plasmonic lens and the incident angle  $\theta$ .

<sup>a)</sup>Current address: Department of Physics and Astronomy, Trinity University, One Trinity Place, San Antonio, TX 78212.

<sup>b)</sup>Author to whom correspondence should be addressed; electronic mail: Xiang@berkeley.edu

$$x = \frac{Rk_{in}}{\sqrt{k_{sp}^2 - k_{in}^2}}. \quad (2)$$

Thus  $x$  is independent of  $\alpha$ , and all SPPs from the circular slit will focus at one point.  $x$  is much smaller than  $R$  when  $k_{in}$  is much smaller than  $k_{sp}$ , i.e., a small incident angle. Therefore, for a plasmonic lens of radius  $R$ , the focus point of SPPs can be well controlled either by changing a small incident angle close to normal or by varying the wavelength of excitation light or combining both methods. This is very similar to paraxial approximation in conventional lens.

The optical response of the plasmonic lens was modeled using MICROWAVE STUDIO™ (MWS), a computer program that calculates the electromagnetic response of metallic and dielectric objects using a method based on the finite difference time domain theory. Silver is used in this study due to its relatively low loss in optical range. Due to the computation limit of MWS, a silver disk of 6  $\mu\text{m}$  in diameter was simulated instead of a circular slit cut into a silver slab. The single edge of the disk will diffract light similar to the double edges slit on a film, especially when the slit width is subwavelength. Both an edge and a slit can be modeled as a line source of SPPs with similar relative electromagnetic field distributions.<sup>11</sup> The absolute field intensity, however, is likely to be different due to the difference in coupling efficiency of the incident light into SPPs. The silver thickness is 200 nm, which is enough to block direct transmission of the incident light. The Drude model,  $\epsilon_r(\omega) = \epsilon_\infty - \{\omega_p^2 / [\omega(\omega - iV_c)]\}$ , is used to describe silver, where the parameters,  $\epsilon_\infty = 6.0$ ,  $\omega_p = 1.5 \times 10^{16}$  rad/s, and  $V_c = 7.73 \times 10^{13}$  rad/s, are obtained by fitting the model to the experimental data (400–550 nm) taken from the literature.<sup>15</sup>

Figure 2 shows the total electric field distribution 20 nm above the silver plasmonic lens. Under normal illumination of 514 nm, SPPs are focused to the center where the electric field is highly concentrated under normal illumination. Since coherent SPPs inevitably experience interference when they cross each other, the focus profile is modulated by interference fringes. The focus spot size is therefore determined by SPP interference to the order of one-quarter of the SPP wavelength, which is much smaller than the excitation light wavelength.<sup>8,10,11</sup> The contribution from the reflected SPPs is negligible because of the very low SPP reflectivity from the disk edge.<sup>16,17</sup> When the incident angle is changed from  $0^\circ$  to  $20^\circ$ , the focus position shifts about 1  $\mu\text{m}$  from the center, which agrees very well with the estimated 1.08  $\mu\text{m}$  from Eq. (2). The SPPs focus point is found independent of polarization, while overall field distribution depends on the excitation polarization, as can be seen in Figs. 2(b) and 2(c). Different polarized illumination excites SPPs at different portions of the edge, but the focus point is only determined by the in-plane momentum, which is not related to polarization. This is also apparent from Eq. (2).

Like conventional three-dimensional (3D) optical lenses, a plasmonic lens follows similar geometric relations that apply to the shorter wavelength of surface plasmon waves; the relationship between focus position and incident angle can also be understood in classical ray optics. In Fig. 2(c), a beam incident to the metal surface at an angle can excite the surface plasmon waves with a phase lag  $d$  on two opposite edges, resulting in a shift of the focus where the optical path lengths (OPL) are equal, i.e.,  $\text{OPL}_{AD} = \text{OPL}_{BC} + \text{OPL}_{CD}$ . This is similar to the conventional lens shown in Fig. 2(d).

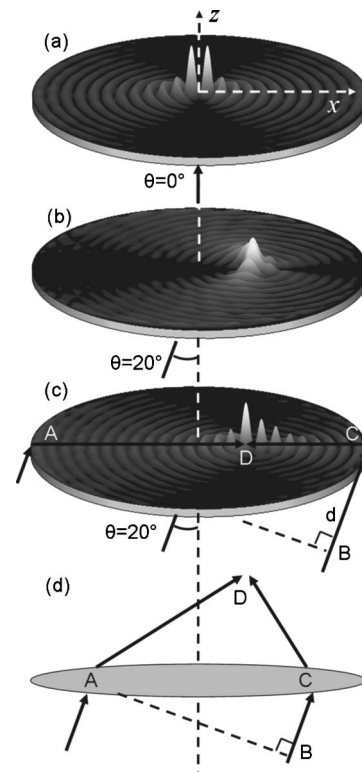


FIG. 2. (a)–(c) MWS simulation of the electrical field intensity distributions of a plasmonic lens with different incident angles and incident polarizations. The diameter of the simulated plasmonic lens is 6  $\mu\text{m}$ . The excitation wavelength is 532 nm in a vacuum. (a) Normal incident with x polarization; (b)  $20^\circ$  incident angle with y polarization; (c)  $20^\circ$  incident angle with x polarization; (d) A schematic illustration of light focusing by a conventional optical lens.

The plasmonic lens was fabricated by depositing a 200 nm silver film onto a quartz substrate and by milling a 250 nm wide slit using FEI Strata 201 XP focused ion beam. A laser (Lambda Pro 120 mW DPSS) with 532 nm wavelength was used for excitation illumination. To visualize the spatial SPP field distribution, we utilized fluorescence imaging.<sup>5,18</sup> Fluorescent molecules were placed in the near field of the silver surface so that they are able to convert evanescent SPPs into propagating fluorescence light. Assuming the quantum efficiency of the fluorescent molecules is constant, the fluorescent light intensity should be proportional to that of SPPs. Rhodamin 6 G molecules were used in our experiments. A  $10^{-4}M$  solution of Rhodamin 6 G was prepared by mixing the molecules with polymethyl methacrylate (PMMA, 495 A4 by Microchem). The resulting solution is spin coated on the sample with a uniform thickness of 150 nm. Then the fluorescence images are finally captured through an optical microscope [Zeiss Axiovert mat 200,  $50\times$  objective, numerical aperture (NA) equal to 0.5] and an edge filter (cutoff wavelength, 534 nm) by a digital camera. The spatial resolution of the fluorescence image is limited by the NA of the optical microscope so that the fringes due to SPP interference were not resolved. However, this method is sufficient to elucidate the overall intensity distribution, thus the focusing properties of the plasmonic lens, by adjusting the incident angle.

Figure 3 shows some of the observed fluorescence images from one plasmonic lens with 10  $\mu\text{m}$  diameter using different polarization and incident angles. If the excitation light is normal [Fig. 3(a)], the SPPs are focused at the center

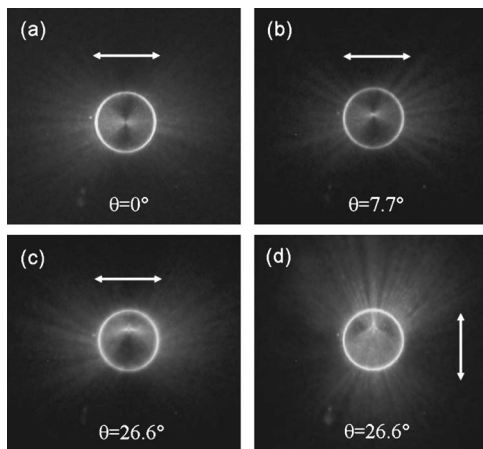


FIG. 3. Fluorescence images observed by optical microscope under different incident angles and polarizations. (a) Normal incident with horizontal polarization; (b)  $7.7^\circ$  incident angle with horizontal polarization; (c),(d)  $26.6^\circ$  incident angle with horizontal and vertical polarization, respectively. The polarization directions are indicated by the double-side white arrows. The incident direction is upwards.

of the lens, thus significantly enhancing the local field intensity. The focus of the lens shifts upwards slightly when the incident light inclines with a small angle [Fig. 3(b)]. The focusing quality does not change significantly when compared with normal incident. By increasing the incident angle to a relatively larger value [Figs. 3(c) and 3(d)], the focal point is shifted further from the center but the focus starts to deteriorate, similar to what happens for a conventional lens in ray optics. Monochromatic aberrations appear when the paraxial approximation is no longer held. Figures 3(c) and 3(d) also show that the focus position does not depend on the polarization, consistent with the numerical simulations in Fig. 2 and Eq. (2). If we compare two plasmonic lenses with different sizes but identical illumination configuration in Fig. 4, the relative focus positions, i.e.,  $x/R$ , for each plasmonic lens are the same. The larger size plasmonic lens will then have a larger displacement of the focus that is predicted by Eq. (2).

All of the above-mentioned focusing properties for the plasmonic lens are very similar to those of a conventional optical lens except for two major differences. First, the plasmonic lens is a two-dimensional element where energy transport and the lens itself are in the same plane, in contrast with conventional 3D optics. The two-dimensional optical process may be useful for the future of integrated photonics. Second, the optical components such as the lens and focus spot size can be well below the free-space diffraction limit, making it an excellent candidate for ultrasmall photonics. In fact, the focus size is only limited by the SPP diffraction limit, which is in order of one-half of the SPP wavelength. In addition, considering the enchantment of SPP, considerably high field density at the focus is also achievable. This is of special importance for some field-enhanced sensing schemes with high spatial resolution, such as surface-enhanced Raman scattering and second harmonic generation.

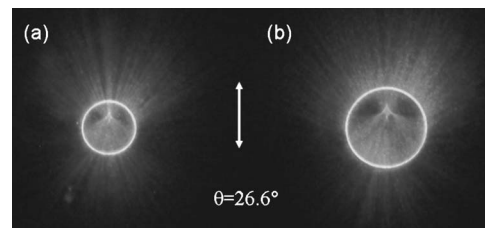


FIG. 4. Fluorescence images observed by optical microscope for two different plasmonic lenses (diameter: 10 and 15  $\mu\text{m}$ , respectively) using exactly the same illumination configuration. The excitation light incident angle is  $26.6^\circ$ . The polarization directions are indicated by the double-side white arrows.

In summary, we have demonstrated that the focal position of a plasmonic lens can be tuned by changing the incident angle of the incident beam. Both the simulation and experimental results reveal that the focusing properties of the silver slit plasmonic lenses are very similar to focusing lenses in conventional optics, except that the foci are extremely close to the lens surface and that subwavelength focusing can be obtained. The focus tunable plasmonic lens has a potential in ultrasmall optical circuits and biological applications.

This work was supported by the U.S. Air Force Office of Scientific Research MURI program under Grant No. FA9550-04-1-0434.

- <sup>1</sup>W. L. Barnes, A. Dereux, and T. W. Ebbesen, *Nature (London)* **424**, 824 (2003).
- <sup>2</sup>F. Keilmann, K. W. Kussmaul, and Z. Szentirmai, *Appl. Phys. B: Photophys. Laser Chem.* **47**, 169 (1988).
- <sup>3</sup>A. Bouhelier, Th. Huser, H. Tamaru, H.-J. Guntherodt, D. W. Pohl, F. I. Baida, and D. Van Labeke, *Phys. Rev. B* **63**, 155404 (2001).
- <sup>4</sup>J.-C. Weeber, J. R. Krenn, A. Dereux, B. Lamprecht, Y. Lacroute, and J. P. Goudonnet, *Phys. Rev. B* **64**, 045411 (2001).
- <sup>5</sup>H. Ditlbacher, J. R. Krenn, G. Schider, A. Leitner, and F. R. Aussenegg, *Appl. Phys. Lett.* **81**, 1762 (2002).
- <sup>6</sup>H. Ditlbacher, J. R. Krenn, A. Leitner, and F. R. Aussenegg, *Opt. Lett.* **29**, 1408 (2004).
- <sup>7</sup>J. C. Weeber, Y. Lacroute, A. Dereux, E. Devaux, T. Ebbesen, C. Girard, M. U. Gonzalez, and A. I. Baudrion, *Phys. Rev. B* **70**, 235406 (2004).
- <sup>8</sup>L. Yin, V. K. Vlasko-Vlasov, J. Pearson, J. M. Hiller, J. Hua, U. Welp, D. E. Brown, and C. W. Kimball, *Nano Lett.* **5**, 1399 (2005).
- <sup>9</sup>A. Drezet, A. L. Stepanov, H. Ditlbacher, A. Hohenau, B. Steinberger, F. R. Aussenegg, A. Leitner, and J. R. Krenn, *Appl. Phys. Lett.* **86**, 074104 (2005).
- <sup>10</sup>Z. W. Liu, Q. H. Wei, and X. Zhang, *Nano Lett.* **5**, 957 (2005).
- <sup>11</sup>Z. W. Liu, J. M. Steel, W. Srituravanich, Y. Pikus, C. Sun, and X. Zhang, *Nano Lett.* **5**, 1726 (2005).
- <sup>12</sup>S. A. Maier, M. D. Friedman, P. E. Barclay, and O. Painter, *Appl. Phys. Lett.* **86**, 071103 (2005).
- <sup>13</sup>H. Raether, *Surface Plasmons on Smooth and Rough Surfaces and on Gratings* (Springer, Berlin, 1988).
- <sup>14</sup>D. Egorov, B. S. Dennis, G. Blumberg, and M. I. Haftel, *Phys. Rev. B* **70**, 033404 (2004).
- <sup>15</sup>P. B. Johnson and R. W. Christy, *Phys. Rev. B* **6**, 4370 (1972).
- <sup>16</sup>J. Seidel, S. Grafstrom, L. Eng, and L. Bischoff, *Appl. Phys. Lett.* **82**, 1368 (2003).
- <sup>17</sup>A. Bouhelier, T. Huser, J. M. Freyland, H.-J. Guntherodt, and D. W. Pohl, *J. Microsc.-Oxf.* **194**, 571 (1999).
- <sup>18</sup>H. Ditlbacher, J. R. Krenn, N. Felidj, B. Lamprecht, G. Schider, M. Salerno, A. Leitner, and F. R. Aussenegg, *Appl. Phys. Lett.* **80**, 404 (2002).